Surface-enhanced Raman scattering for the rapid discrimination of bacteria

Roger M. Jarvis,[a] Alan Brooker[b] and Royston Goodacre*[a]

Received 9th May 2005, Accepted 13th May 2005
First published as an Advance Article on the web 29th September 2005
DOI: 10.1039/b506413a

Raman spectroscopy is attracting interest for the rapid identification of bacteria and fungi and is now becoming accepted as a potentially powerful whole-organism fingerprinting technique. However, the Raman effect is so weak that collection times are lengthy, and this insensitivity means that bacteria must be cultured to gain enough biomass, which therefore limits its usefulness in clinical laboratories where high-throughput analyses are needed. The Raman effect can fortunately be greatly enhanced (by some 10^3–10^6-fold) if the molecules are attached to, or microscopically close to, a suitably roughened surface; a technique known as surface-enhanced Raman scattering (SERS). In this study we investigated SERS, employing an aggregated silver colloid substrate, for the analysis of a closely related group of bacteria belonging to the genus *Bacillus*. Each spectrum took only 20 s to collect and highly reproducible data were generated. The multivariate statistical technique of principal components-discriminant function analysis (PC-DFA) was used to group these bacteria based on their SERS fingerprints. The resultant ordination plots showed that the SERS spectra were highly discriminatory and gave accurate identification at the strain level. In addition, *Bacillus* species also undergo sporulation, and we demonstrate that SERS peaks that could be attributed to the dipicolinic acid biomarker, could be readily generated from *Bacillus* spores.

1 Introduction

The near infrared (NIR) Raman effect is rather weak as approximately only 1 in 10^6 incident photons are Raman shifted.[1] For analysis of complex biological samples, which tend to be weak Raman scatterers, it is even more difficult to acquire good Raman spectra without resorting to lengthy collection times. However, a number of enhancement methods are available that can significantly increase the cross-section of Raman spectra. Perhaps two of the most popular techniques are ultraviolet resonance Raman (UVRR) enhancement and surface-enhanced Raman scattering (SERS). The resonance Raman effect can increase intensities by several orders of magnitude and typically requires incident radiation at ultra-violet frequencies.[2] With SERS, enhancements of some 10^4–10^6 fold, and even up to 10^{14} have been demonstrated for certain analytes.[3–5] This method makes use of a metal surface with special properties that gives rise to increased intensities.

Deep UVRR was the first Raman technique to yield Raman spectra that showed promise for use in microbial analysis.[6–8] However, due to photochemical or 'burning' effects, caused by the highly energetic nature of UV photons, and the comparative expense of UV Raman systems, little development has taken place. Work that followed the earlier experiments in the 1980s investigated the detection of small numbers of bacteria and bacterial spores, the effect of bacterial cultural conditions on UVRR spectra and has also thoroughly studied the spectra resulting from a range of cellular structures.[6,7,9–14] More recently, bacterial discrimination using deep UVRR with

[a] *School of Chemistry, The University of Manchester, PO Box 88, Sackville St, Manchester, UK, M60 1QD. E-mail: Roy.Goodacre@manchester.ac.uk; Fax: +44 (0) 161 306 4519; Tel: +44 (0) 161 306 4480*
[b] *Renishaw plc, Old Town, Wotton-under-Edge, Gloucestershire, UK, GL12 7DW*

chemometrics has been demonstrated for bacterial species level discrimination[15a,16] the analysis of the mode-of-action of antibiotics,[15b] and for bioprocess monitoring.[17]

The second Raman enhancement method which has been gaining increasing popularity for biological analysis is SERS. The technique relies on either the adsorption or close proximity of an analyte to a metal substrate.[18,19] The substrate can take the form of a roughened metal surface, a colloidal solution or a roughened electrode. The total enhancement of the SERS effect is explained by two processes; a charge transfer mechanism, known as chemical enhancement; and an electromagnetic enhancement effect.[3,20] In addition to signal enhancement, SERS exhibits a fluorescence quenching effect.[21] This is extremely useful when examining microorganisms, which often generate a high fluorescence background under excitation in the near infra-red to visible regions of the electromagnetic spectrum. Moreover, since SERS has only been shown to be effective under IR or visible excitation there are no drawbacks associated with photochemical degradation of the sample as in UVRR. SERS has received much attention recently within biomedicine and genomics,[22] and is emerging as a very powerful (bio-)chemical detection method.[15b,23,24]

Several investigations into SERS of bacteria have been undertaken.[25–29] The first report of bacterial SERS spectra by Efrima & Bronk[25] used a sodium borohydride reduced silver colloid at 514.5 nm excitation. Although little difference between SERS from the surface of (bio-)chemically diverse Gram-positive and Gram-negative bacteria was noted. However, more recent reports have shown that SERS, under different conditions to those reported by Efrima, can be used for the purpose of bacterial discrimination, and has the potential to significantly reduce spectral collection times for such experiments from minutes to just a few seconds.[30–33]

There is also a great deal of interest in methods that can be used for the rapid detection of low concentrations of bacterial spores, especially for those from *Bacillus anthracis*, the causal agent of anthrax. With its especially acute sensitivity and relative inexpensiveness, SERS is very promising as a method for the detection of these biological agents. Common to the bacterial spore across *Bacillus* and *Clostridium* species is the presence of a large proportion (1–14%) of dipicolinic acid (DPA). This can be used as a potential biomarker for the detection of spores, and therefore much interest has been shown in the use of physico-spectroscopic methods to detect this chemical directly.[10,14,34–38] Amongst the recent literature in this field are two reports of the use of SERS for the detection of bacterial spores, based on the DPA biomarker. Bell *et al.*[34] were able to optimise the quantification of a range of DPA dilutions between 0–50 ppm using SERS. In a more recent study, Zhang and co-workers[35] demonstrated a portable SERS biosensor for the detection of bacterial spores, once again targeting the DPA biomarker.

2 Materials and methods

2.1 Bacterial strains and growth conditions

2.1.1 Comparison of Gram-negative and Gram-positive species by SERS. Three laboratory strains, one each of *Escherichia coli* (strain UB5201), *Bacillus subtilis* (the type strain B0014^T) and *Staphylococcus aureus* (Oxford strain) were analysed by SERS. The isolates were cultivated axenically and aerobically for 16 h at 37 °C on LabM blood agar base (IDG Plc, Lancashire, U.K.). After subculturing three times, each strain was grown on four individual Petri dishes to give four biological replicates of each strain. Biomass was then carefully collected from single colonies on each dish using sterile plastic inoculating loops. This material was added to 100 μl aliquots of silver colloid with 50 μl of 0.01 M NaCl (99.9%, Fisher Scientific, Leicestershire, U.K.) aggregating agent, before spotting on to a 96 well silicon plate (Bruker Ltd, Coventry, U.K.).

2.1.2 Characterisation of *Bacillus* isolates. A collection of nine strains known to belong to the *Bacillus* genera were used in this study (see Table 1). All isolates were cultivated as described above, and once again four biological replicates of each strain were analysed by SERS.

2.1.3 Detection of bacterial spore biomarkers. The laboratory strain of *B. subtilis* B0014^T was cultured to favour sporulation as described in Goodacre *et al.*[36] Briefly, spores were prepared by incubation on LabM (IDG plc.) blood agar base plates + 5 mg L^{-1} $MnSO_4$ at 30 °C for 7 days.[39] No attempt was made to remove any cell debris or vegetative cells from the spore preparations.

Table 1 The *Bacillus* strains used for SERS fingerprinting

Species	Strain no.	Source	ID
B. amyloliquefaciens	28	Gordon	BA28
B. amyloliquefaciens	29	Goodfellow	BA29
B. amyloliquefaciens	32	Gordon, LMG 12324	BA32
B. amyloliquefaciens	30	Gordon	BA30
B. licheniformis	18	Logan	BL18
B. licheniformis	20	Bristol	BL20
B. subtilis	10	DSM	BS10
B. subtilis	6	Spore strip, Halls	BS6
B. subtilis	8	Gibson	BS8

2.2 Silver colloid preparation

A batch of citrate reduced silver colloid was prepared by a modified Lee & Meisel[40] method similar to that described by Munro *et. al.*[41] A conical flask containing 100 ml of distilled water was heated to a temperature of 45 °C with continuous stirring, at which point 18 mg of $AgNO_3$ (>99%, Sigma, Dorset, U.K.) suspended in 2 ml of distilled water was added. With further heating and stirring the solution was brought to boiling point and 2 ml of 1% (w/v) trisodium citrate (99.66%, Fisher Scientific, Leicestershire, U.K.) introduced to the flask. The solution was boiled for 10 min, allowing sufficient time for formation of the colloidal particles. This was noted by the gradual colour change from a colourless to a grey/green solution approximately 5 min after addition of the trisodium citrate. The flask was taken off the heat and cooled rapidly in an ice bath to quench any further reaction.

2.3 Raman microscopy

SERS spectra were collected using a Renishaw 2000 Raman microscope (Renishaw plc., Old Town, Wotton-under-Edge, Gloucestershire, UK) with a low power (24 mW) near infrared 785 nm diode laser with power at the sampling point $\sim$10 mW.[42,43] The instrument was wavelength calibrated with a silicon wafer focused under the $\times$50 objective and collected as a static spectrum centred at 520 cm^{-1} for 1 s.

The samples, dried at 50 °C for 15 min, were presented on a 96 well silicon plate. The motorised *xy*-stage was programmed to read the plate and for each measurement a bacterial SERS spectrum was collected using an $\times$20 objective lens for a single 20 s accumulation. Four 'biological replicates' were analysed, meaning that samples were taken from four freshly prepared bacterial culture plates on different days and four spectra collected as detailed above.

The GRAMS WiRE software package (Galactic Industries Corporation, 395 Main Street, Salem, NH, USA) running under Windows 95 was used for instrument control and data capture. Stokes Raman spectra were collected between a wavenumber range of $\sim$600–1600 cm^{-1} with a spectral resolution of $\sim$6.5 cm^{-1}. Each sample was represented by a spectrum containing 1064 points and spectra were displayed in terms of the Raman scattered photon count (see Fig. 1 for examples).

ASCII data were exported from the GRAMS WiRE software into MATLAB version 6 (The Math Works, Inc., 24 Prime Par Way, Natick, MA, USA). To address baseline differences the spectra were normalised so that the peak with the greatest magnitude was set to a value of +1.

2.4 Structural and chemical analyser

Renishaw's structural and chemical analyser (SCA) has been described in detail previously.[30] This Raman interface to a scanning electron microscope (SEM) enables laser light to be focused onto a micrometer order sized spot, which is governed by the diameter of the laser beam. Raman spectra can then be collected from this spot, whilst maintaining the ability to view the secondary electron image (SEI). The imaging power of the SEM can be used to identify regions of interest on samples; these can then be analyzed using Raman spectroscopy.

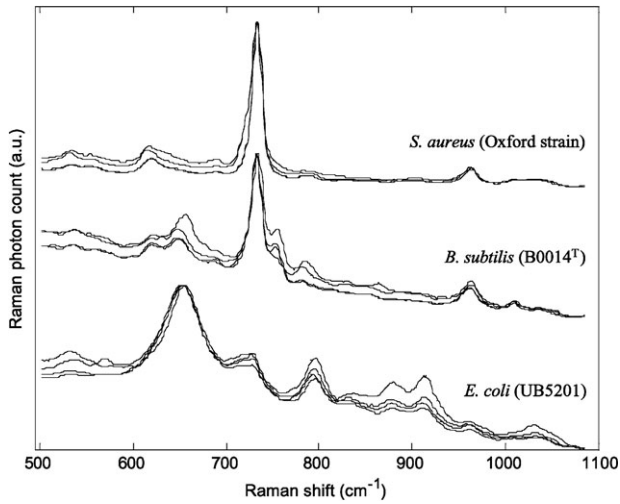

Fig. 1 SERS spectral fingerprints taken from laboratory strains of *Staphylococcus aureus* (Oxford strain), *Bacillus subtilis* (B0014^T) and *Escherichia coli* (UB5201). Each of the four biological replicate spectra are shown.

A JEOL JSM-5610LV SEM was used to observe the samples. SEMs work by focussing an energetic (1–25 keV) electron beam onto the sample; typically, secondary electrons are detected for each point on the sample and this signal is then used to build up an image. The magnification can be altered by changing the scanned area on the sample. SEM has a number of advantages over optical microscopy, principally greater spatial resolution and depth of field, and normally better discrimination due to a range of contrast mechanisms.

2.5 Cluster analysis

Cluster analysis was performed in MATLAB as previously reported.[44] Briefly, principal components analysis (PCA[45]) was used to reduce the dimensionality of the SERS data prior to discriminant function analysis (DFA[46]). DFA then discriminated between groups on the basis of these retained PCs (the numbers used and the percentage explained variance are detailed in the figures) and the *a priori* knowledge of which spectra were the biological replicates. DFA was programmed to maximise the Fisher ratio (*i.e.*, the within-class to between-class variance) and the spectral similarity between different classes reflects the optimal number of PCs that are fed into the DFA algorithm.[46] The number of PCs used for DFA were determined using the parsimony principle,[47] by extracting the fewest number of PCs that showed maximal class separation.

For model validation the method of data splitting (also known as full cross-validation) was used.[48] This approach works by splitting the measured samples in to two groups; a model *training* and *independent test* set. The model is trained on the first set and then tested for accuracy on the second set of 'hold-out' data. Using this method of validation in conjunction with the principle of parsimonious data modelling ensures that the model is not over trained, and therefore is general enough for subsequent predictions on unknown or additional samples.

3 Results and discussion

3.1.1 Comparison of Gram-negative and Gram-positive bacteria by SERS

As an initial step to gain an understanding of how SERS spectra differ between different bacterial Gram types, the small set of laboratory isolates were analysed by SERS. In Fig. 1, the SERS spectrum for each biological replicate is plotted. It can be seen from this figure that the spectral reproducibility is very good for these data, although quantitative differences are apparent for both *B. subtilis* and *E. coli*. It is likely that these differences are in most part due to inconsistencies arising

from the SERS technique, rather than any significant biological dissimilarity between biological replicates, as can be judged from previous studies.[31]

There are obvious differences in the spectral profiles between each of the species. The most marked difference can be seen between the Gram-negative *E. coli* and the Gram-positive *B. subtilis* and *S. aureus*. The latter two share a strong band at $\sim$730 cm^{-1}, most likely attributable to a glycosidic ring vibration arising from the presence of polysaccharides on the cell surface,[31,33] whereas for *E. coli* this region is represented by a broad, weak peak. These observations are reflected in the PCA scores plot (Fig. 2) derived from these spectra, where the closeness between the biological replicate spectra of each strain confirms that a very high degree of reproducibility can be achieved with SERS across the whole spectral range from 600–1600 cm^{-1}. In addition, there is separation between the Gram-negative *E. coli* and the two Gram-positive strains along the first principal component (PC), which accounts for 91.7% of the variance within the data. Along the second PC, which accounts for much less of the total variance in the spectra (only 6.5%), a clear distinction is also shown between the two Gram-positive bacterial strains of *B. subtilis* and *S. aureus*.

Applying SERS to the study of bacterial cells, using the method described here means that mainly the biochemistry of the bacterial cell surface is being probed by the technique.[31] Therefore, the differences between the Gram-positive and Gram-negative organisms that are reflected in their SERS spectra should be related back directly to their cell wall structures. In Fig. 3, cartoons of the cell walls of each of the two organism Gram types are shown. The Gram-positive cell wall, represented in Fig. 3A consists of a thick outer layer of peptidoglycan, a matrix of complex carbohydrates of *N*-acetyl-D-glucosamine (NAD) and *N*-acetylmuramic acid (NAM) linked by peptide bridges. Bound to the peptidoglycan layer are units of teichoic or teichuronic acid, which consist of sugars and amino acid groups. This tough outer layer shields the cytoplasmic membrane which is formed from phospholipids and proteins and allows for active transport of nutrients across the cell barrier.

By contrast, the cell wall of Gram-negative organisms (Fig. 3B) has a much thinner layer of peptidoglycan; but possesses an additional structure, or outer membrane, which is rich in lipopolysaccharides (LPSs). The outer membrane is packed with proteins called porins for the passive diffusion of nutrients across the cell membrane; long chain carbohydrates also project from the cell surface, anchored to lipid A of the LPS. The peptidoglycan layer resides within the periplasmic space which is located between the inner and outer membranes. The cytoplasmic (inner) membrane forms the final barrier to the interior of the cell.

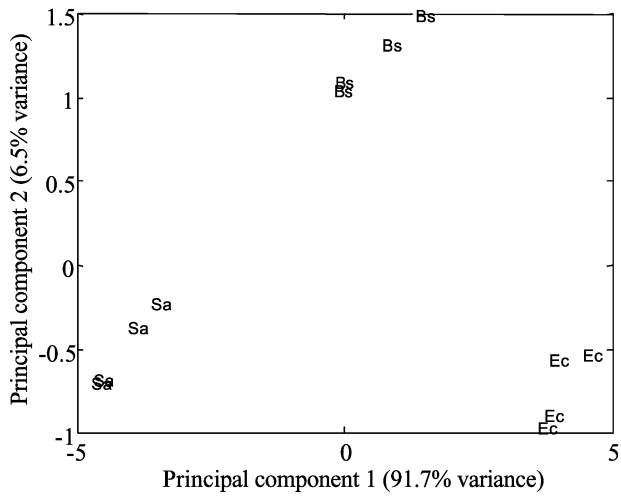

Fig. 2 A PCA ordination plot showing the excellent experimental reproducibility obtained for SERS from the bacterial laboratory strains. In addition, separation between the Gram-positive and Gram-negative species is achieved along the first principal component, which accounts for a majority of variance in the data.

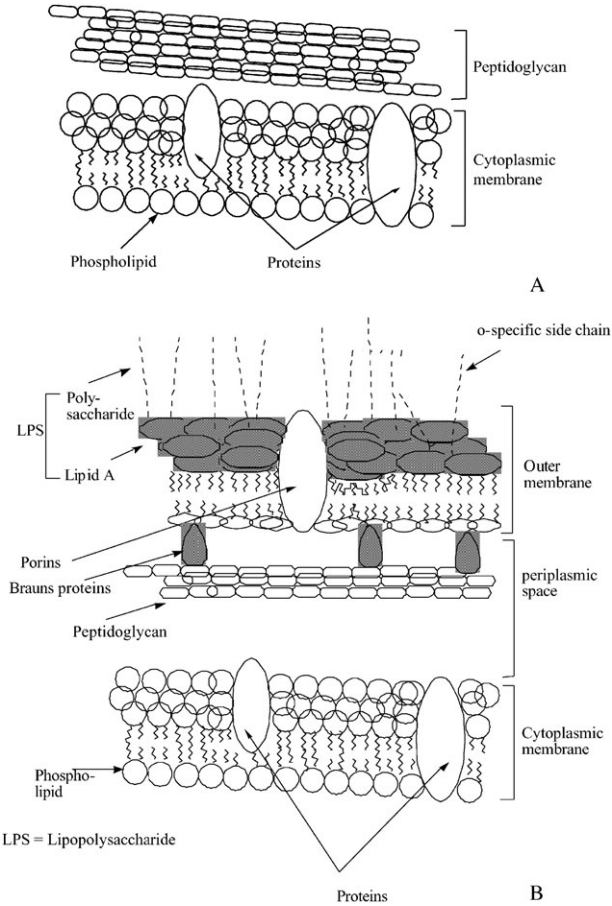

Fig. 3 (A) A depiction of the cell wall of a Gram-positive prokaryotic bacterium. The peptidoglycan membrane, which is targeted by SERS, is composed of the complex carbohydrates *N*-acetylmuramic acid (NAM) and *N*-acetyl-D-glucosamine (NAG). (B) A diagram demonstrating the structure of the Gram-negative cell wall.

The inference of these structural differences is that SERS spectra acquired from Gram-positive bacteria are likely to be similar since there appears to be less chemical differences manifest there, and Fig. 1 (and indeed the other *Bacillus* SERS spectra detailed below) suggest this to be true. Therefore it is likely that using SERS to discriminate between Gram-positive *Bacillus* will be more challenging as the spectra will be less descriptive of an organisms phenotype than spectra obtained from Gram-negative bacteria. Indeed as reported in ref. 31 who studied predominantly Gram-negative bacteria associated with urinary tract infection, many of the SERS spectra from different bacterial species could be readily discriminated by eye.

3.1.2 Characterisation of *Bacillus* isolates

The main purpose of this present study was to apply SERS fingerprinting to the more challenging task of discriminating between Gram-positive bacteria, in particular strains belonging to the *Bacillus* genera. This group of organisms is particularly important for several reasons; in particular, due to the current social and political climate there is much interest in bacilli, since the *B. anthracis* pathogen is one of the members of this group. Thus speedy detection of this bacterium is important for preventing acts of bio-terrorism[49] and SERS could potentially play a role here.[33–35] Secondly, no

detailed investigation in to the discrimination of *closely* related Gram-positive species has been conducted using SERS; indeed, the ability of the method to be applied to species level discrimination has yet to be shown.

Therefore, in this study three closely related and well documented species of *Bacillus* bacteria were analysed by SERS,[15,36,50] these bacteria all belong to the very closely related *Bacillus subtilis* group, which is hard to discriminate between using genetic methods,[15] and include *B. subtilis*, *B. amyloliquefaciens* and *B. licheniformis*. In Fig. 4, the SERS spectra collected from four isolates of *B. amyloliquefaciens* are plotted; these spectra and indeed the others discussed below are raw, and have merely been scaled to unity with respect to the band at 732 cm^{-1}. Across the four biological replicates of each isolate the spectral reproducibility is very good, with subtle quantitative differences noticeable for replicate spectra of each isolate, with the exception BA30. For instance, a single replicate of the BA32 isolate has an additional peak at 851 cm^{-1}, a replicate of BA29 has a relatively strong peak at 1283 cm^{-1}, whilst a single replicate of BA28 exhibits a peak at 905 cm^{-1}. In quantitative terms, the relative intensities of the bands at 732 cm^{-1} and 1050 cm^{-1} show reproducible differences between the bacterial isolates, therefore some clear discriminatory information between sub-species exists.

For the biological replicate spectra of the two isolates of *B. licheniformis* studied (Fig. 5), the qualitative reproducibility of the spectra is far better than for *B. amyloliquefaciens*, however, once again quantitative differences are noticeable for the bands in the 600–800 cm^{-1} region. Direct comparison of the *B. amyloliquefaciens* spectra against those of *B. licheniformis* reveals clear quantitative differences in the *B. licheniformis* Raman bands above $\sim$1000 cm^{-1}, which are far stronger than their counterparts in the *B. amyloliquefaciens* spectra.

Finally, for the SERS spectra of *B. subtilis* plotted in Fig. 6, the greatest within species and between species spectral differences can be seen. Firstly, from comparison of the SERS spectra of the three *B. subtilis* isolates, BS8 stands out from BS6 and BS10, with a far greater relative intensity for the band at 732 cm^{-1}. In addition, the intensity of the broad peak at 1330 cm^{-1} is greater than that of the same band in the SERS spectra of BS6 and BS10. There are also clear differences in the relative intensities of the peaks at 626 cm^{-1} and 662 cm^{-1}; for BS8 these bands have similar intensities, whereas for the two other strains the magnitude of the more greatly shifted peak is far larger. The most obvious difference between these *B. subtilis* SERS spectra and those of the other bacilli is in the presence of a weak band at 1001 cm^{-1}, most often attributable to aromatic ring

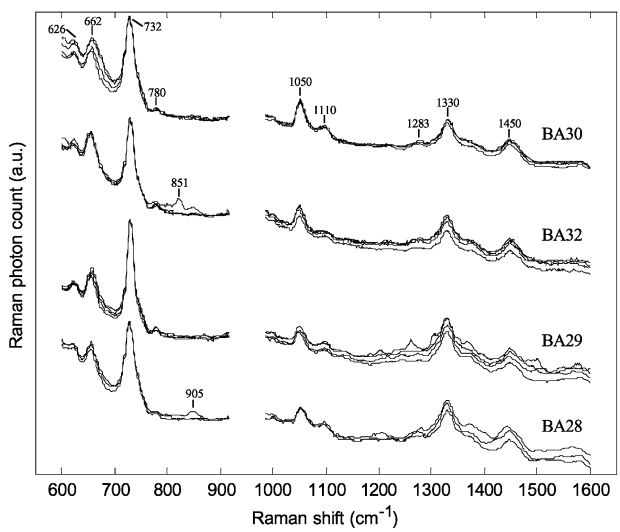

Fig. 4 SERS spectral fingerprints taken from four strains of *B. amyloliquefaciens*, including each of the four biological replicates for each strain. The characteristic peak attributable to Gram positive organisms is present at $\sim$730 cm^{-1}. The region between $\sim$920 cm^{-1} and 980 cm^{-1} was removed for the analysis due to the presence of a broad, weak signal from the silicon plate.

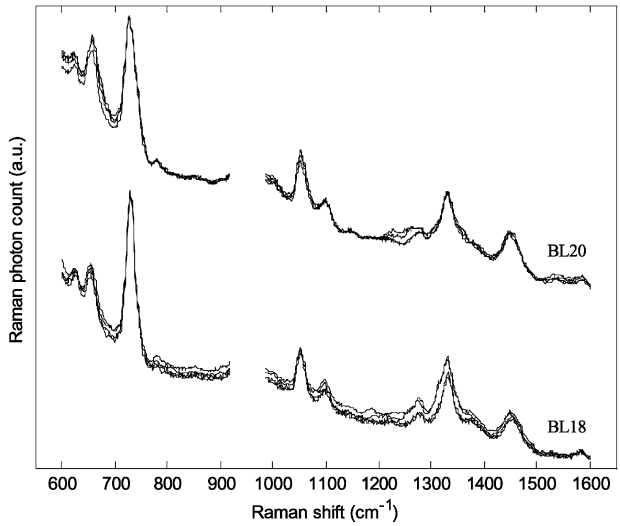

Fig. 5 SERS spectral fingerprints taken from two strains of *B. licheniformis*, including each of the four biological replicates for each strain.

vibrations, and in this instance very likely indicative of detectable levels of one or more of the aromatic amino acids. For BS6 and BS10 the other prominent difference can be seen in the relative magnitudes of the bands at 662 cm^{-1} and 732 cm^{-1}. These peaks have very similar intensities, whereas for all of the other strains analysed the band at 732 cm^{-1} is much more dominant.

At this stage it is rather difficult to make anything other than the most tentative assignments for the peaks identified in these spectra. However, strong evidence from previous work identifies the band at 732 cm^{-1} to be attributable to a vibrational mode of the glycosidic ring present in NAG and NAM[31]. Otherwise, inferences as to the provenance of these Raman bands must be based on the knowledge that SERS is probing the cell surface. For instance, peaks in the region between

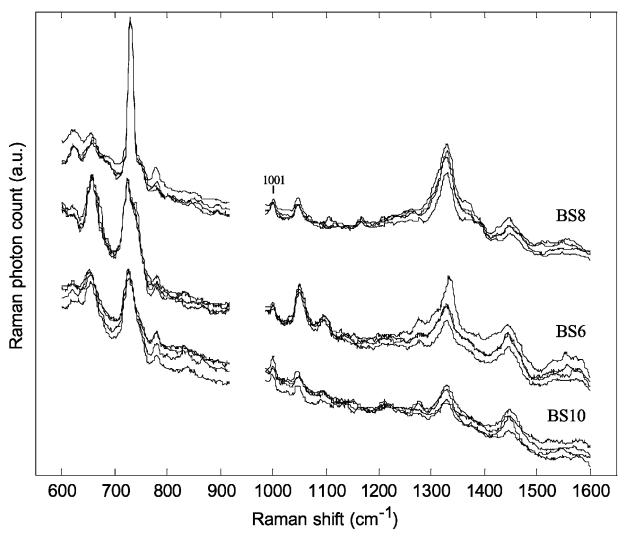

Fig. 6 SERS spectral fingerprints taken from three strains of *B. subtilis*, including each of the four biological replicates for each strain.

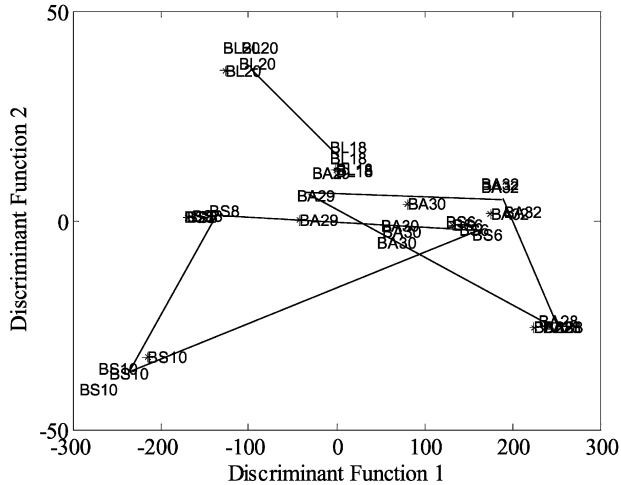

Fig. 7 A cross validated PC-DFA ordination plot derived from the SERS spectra acquired from the 9 strains of *Bacillus* listed in Table 1. The validation spectra are identified by *. The close proximity of biological replicates in this plot demonstrates the excellent experimental reproducibility achieved by SERS.

930 cm^{-1} and 1130 cm^{-1} have previously been assigned to phospholipids,[51] whilst protein backbone and carboxylic stretches are likely to be found further upstream beyond $\sim$1220 cm^{-1}.[33]

To determine whether these isolates could be separated on the basis of their SERS spectral fingerprints, cluster analysis was applied to the data as described above. Initially, the *unsupervised* approach of PCA was used to reduce the dimensionality of the data from 1064 variables to 7 principal components (PCs), which accounted for 98.7% of the explained variance. These PCs were then processed by the *supervised* DFA clustering algorithm, which used the *a priori* knowledge of the biological replicates to formulate a categorical model to describe the relationship between these isolates, by optimising the ratio of the between-group to within-group variance. In Fig. 7, the resultant cross validated PC-DFA ordination plot is shown. This plot shows that very good separation can be obtained between the bacterial isolates, regardless of species, which suggests that SERS is biased towards providing sub-species sensitivity for these organisms. Note also that the projected test set SERS spectra (those marked with an *) are superimposed on the training clusters, highlighting the excellent reproducibility across the full set of SERS spectra. However, as indicated by the lines drawn on the plot there is some separation between species, where *B. subtilis* (with the exception of BS8) can be distinguished from both *B. amyloliquefaciens* and *B. licheniformis* along the first discriminant function (DF). Whilst *B. licheniformis* separates from both *B. subtilis* and *B. amyloliquefaciens* along the 2nd DF. Given the spectral differences and similarities described above, it is apparent why definitive separation between species is not recovered by cluster analysis.

3.1.3 Detection of bacterial spores using SERS

Members of the genus *Bacillus* are aerobic endospore-forming bacteria that undergo sporulation when nutrients are lacking. The resultant spores are very resilient to chemical and physical stresses which allows for their survival over 100s of years. This physiological change is an important part of the life cycle of *Bacillus* (and indeed *Clostridium*) and the detection of spores is important in food processing laboratories,[52] as well as in detecting its potential use as a biological warfare agent.[53]

The purpose of this exercise was to demonstrate the application of the SCA to the analysis of bacterial spores by SERS. Fig. 8 shows SEM images acquired from *B. subtilis* $B0014^T$ spores from the region in which the SERS spectrum in Fig. 9B was collected. The image in the background was taken at the same magnification at which the SCA is operated for collection of Raman or SERS spectra ($\times$1000). Sample charging effects are obvious at this magnification, although imaging in SEI mode greatly reduces this problem. The inset higher magnification ($\times$4000) image represents the

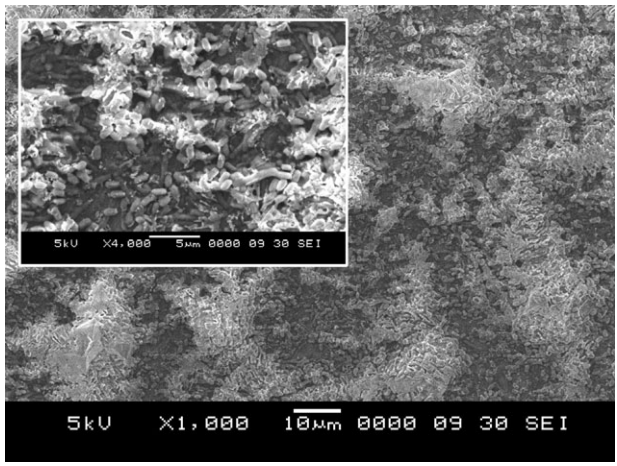

Fig. 8 SEM image of sporulated *B. subtilis* B0014^T cells, showing ellipsoidal spores ~ 1 μm in length. The lower magnification image at $\times 1000$ is equivalent to the magnification at which the structural and chemical analyser (SCA) can be operated. The higher magnification image ($\times 4000$; inset), although distorted by charging effects, shows the cell structure more clearly.

maximum magnification that was obtainable for SEM imaging under these conditions. It is clear from this that the cells have sporulated, where as healthy vegetative bacilli are typically $1 \times 2-3$ μm in size, these spores have dimensions of $\sim 1 \times 1$ μm.

In Fig. 9A, the SERS spectrum of a vegetative cell of *B. subtilis*, acquired using the Raman microscope system is shown. This is representative of the spectra obtained previously from *B. subtilis* strains using SERS. Next, in Fig. 9B a SERS spectrum obtained from sporulated cells of B0014^T using the SCA, demonstrates very clear differences between the SERS spectra of

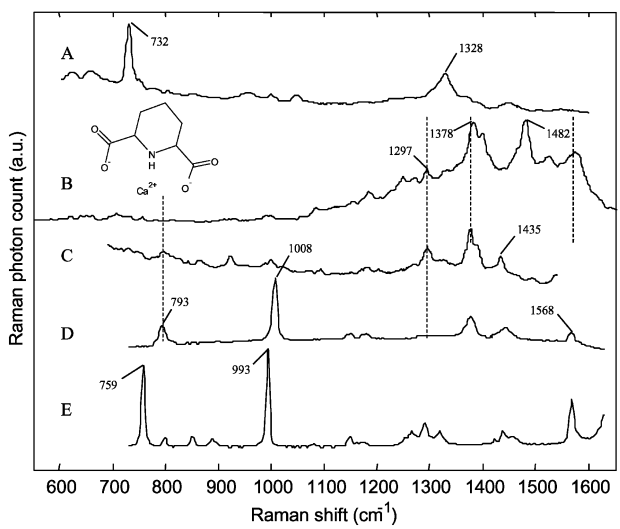

Fig. 9 Spectra of *B. subtilis* B0014^T acquired using 785 nm laser excitation under the following conditions; (A) SERS spectrum of vegetative cells acquired with a Raman microscope; (B) SERS spectrum of sporulated cells acquired with the structural and chemical analyser; (C) SERS spectrum of sporulated cells acquired with the Raman microscope; (D) SERS spectrum of dipicolinic acid (DPA) acquired with the Raman microscope; (E) Raman spectrum of DPA acquired with the Raman microscope. The vertical dotted lines indicate complementary Raman bands within the spore SERS spectra and the DPA SERS spectrum.

sporulated and vegetative *Bacillus* cells. In Fig. 9C, a second SERS spectrum of a spore sample is shown; on this occasion acquired using the Raman microscope system. The SERS spectra in Fig. 9B and 9C both share several major features, including the strong band at 1378 cm^{-1}. This is particularly important since the SERS spectrum of DPA in Fig. 9D also exhibits this band, and therefore under these SERS conditions this peak could provide the biomarker required to detect bacterial spores. It is also encouraging that peaks in this region of the Raman spectrum are known to be representative of carboxylate (CO_2^-) vibrations,[54] which provides further evidence that SERS is detecting bacterial spores in these experiments. Finally, the near infrared Raman spectrum of DPA is plotted in Fig. 9E. This spectrum is quite different to that of its SERS counterpart, it is far richer in Raman bands, which largely appear at different points on the spectrum, and importantly does not have the enhanced carboxylate peak at 1378 cm^{-1} which we believe could be used to detect DPA from spores.

3.1 Conclusions

In this study we investigated SERS, employing an aggregated silver colloid substrate, for the analysis of a closely related group of bacteria belonging to the genus *Bacillus*. Highly reproducible spectra were acquired in only 20 s from different strains of *B. subtilis*, *B. amyloliquefaciens* and *B. licheniformis*. All the spectra of these Gram-positive organisms displayed very similar profiles which was in contrast to our previous studies where we analysed Gram-negative bacteria,[31] and we consider that this is likely to be due to the uniformity that is found in the Gram-positive cell wall.

Therefore, the multivariate statistical techniques of principal components-discriminant function analysis (PC-DFA) was used to group these bacteria based on their SERS fingerprints. The resultant ordination plots showed that the SERS spectra were highly discriminatory. This PC-DFA cluster analysis was tested using SERS spectra generated from fresh cultures of bacilli and because the projected test data were recovered wholly congruent with their respective strains, this shows that SERS can be used to give accurate identification at the strain level.

Finally, we also demonstrated that SERS could be used to detect the dipicolinic acid spore biomarker readily from *Bacillus* spores using both SERS on an optical microscope and by targeted collection using a SEM–Raman interface.

In conclusion, we believe that SERS is a very rapid microbiological identification method that should be investigated further for its ability to identify bacteria.

Acknowledgements

RMJ and RG would like to thank the BBSRC for funding. We are also grateful to Dr Catherine Winder for providing Fig. 3.

References

1 N. B. Colthup, L. H. Daly and S. E. Wiberley, *Introduction to Infrared and Raman Spectroscopy*, 3rd edn., Academic Press Limited, London, 1990.
2 P. R. Carey, *Biochemical Applications of Raman and Resonance Raman Spectroscopies*, Academic Press, New York, 1982.
3 M. Moskovits, *Rev. Mod. Phys.*, 1985, **57**, 783–826.
4 S. M. Nie and S. R. Emery, *Science*, 1997, **275**, 1102–1106.
5 K. Kneipp, H. Kneipp, R. Manoharan, E. B. Hanlon, I. Itzkan, R. R. Dasari and M. S. Feld, *Appl. Spectrosc.*, 1998, **52**, 1493–1497.
6 R. A. Dalterio, M. Baek, W. H. Nelson, D. Britt, J. F. Sperry and F. J. Purcell, *Appl. Spectrosc.*, 1987, **41**, 241–244.
7 R. A. Dalterio, W. H. Nelson, D. Britt and J. F. Sperry, *Appl. Spectrosc.*, 1987, **41**, 417–423.
8 K. A. Britton, R. A. Dalterio, W. H. Nelson, D. Britt and J. F. Sperry, *Appl. Spectrosc.*, 1988, **42**, 782–788.
9 R. Manoharan, E. Ghiamati, S. Chadha, W. H. Nelson and J. F. Sperry, *Appl. Spectrosc.*, 1993, **47**, 2145–2150.
10 R. Manoharan, E. Ghiamati, R. A. Dalterio, K. A. Britton, W. H. Nelson and J. F. Sperry, *J. Microbiol. Methods*, 1990, **11**, 1–15.
11 W. H. Nelson, R. Manoharan and J. F. Sperry, *Appl. Spectrosc. Rev.*, 1992, **27**, 67–124.
12 S. Chadha, R. Manoharan, P. Moenne-Loccz, W. H. Nelson, W. L. Peticolas and J. F. Sperry, *Appl. Spectrosc.*, 1993, **47**, 38–43.

13 S. Chadha, W. H. Nelson and J. F. Sperry, *Rev. Sci. Instrum.*, 1993, **64**, 3088–3093.
14 E. Ghiamati, R. Manoharan, W. H. Nelson and J. F. Sperry, *Appl. Spectrosc.*, 1992, **46**, 357–364.
15 (*a*) E. C. Lopez-Diez and R. Goodacre, *Anal. Chem.*, 2004, **76**, 585–591; (*b*) E. C. Lopez Diez, C. L. Winder, L. Ashton, F. Currie and R. Goodacre, *Anal. Chem.*, 2005, **77**, 2901–2906.
16 R. M. Jarvis and R. Goodacre, *FEMS Microbiol. Lett.*, 2004, **232**, 127–132.
17 S. Clarke, R. Littleford, W. Smith and R. Goodacre, *Analyst*, 2005, in press.
18 *Surface Enhanced Raman Scattering*, ed. R. K. Chang and T. E. Furtak, Plenum Press, New York, 1982.
19 M. Fleischmann, P. J. Hendra and A. J. McQuillan, *Chem. Phys. Lett.*, 1974, **26**, 163–166.
20 A. Otto, I. Mrozek, H. Grabhorn and W. Akemann, *J. Phys.-Condens. Matter*, 1992, **4**, 1143–1212.
21 K. Kneipp, A. S. Haka, H. Kneipp, K. Badizadegan, N. Yoshizawa, C. Boone, K. E. Shafer-Peltier, J. T. Motz, R. R. Dasari and M. S. Feld, *Appl. Spectrosc.*, 2002, **56**, 150–154.
22 B. Moore, L. Stevenson, A. Watt, S. Flitsch, N. Turner, C. Cassidy and D. Graham, *Nat. Biotechnol.*, 2004, **22**, 1133–1138.
23 K. Faulds, W. E. Smith and D. Graham, *Anal. Chem.*, 2004, **76**, 412–417.
24 K. Faulds, W. E. Smith, D. Graham and R. J. Lacey, *Analyst*, 2002, **127**, 282–286.
25 S. Efrima and B. V. Bronk, *J. Phys. Chem. B*, 1998, **102**, 5947–5950.
26 N. F. Fell, A. G. B. Smith, M. Vellone and A. W. Fountain, in *Vibrational Spectroscopy-Based Sensor Systems*, 2002, vol. 4577, 174–181.
27 A. A. Guzelian, J. M. Sylvia, J. A. Janni, S. L. Clauson and K. M. Spencer, in *Vibrational Spectroscopy-Based Sensor Systems*, SPIE-Int Society Optical Engineering, Bellingham, 2002, vol. 4577, pp. 182–192.
28 L. Zeiri, B. V. Bronk, Y. Shabtai, J. Czege and S. Efrima, *Colloids Surf., A*, 2002, **208**, 357–362.
29 L. Zeiri, B. V. Bronk, Y. Shabtai, J. Eichler and S. Efrima, *Appl. Spectrosc.*, 2004, **58**, 33–40.
30 R. M. Jarvis and R. Goodacre, *Anal. Chem.*, 2004, **76**, 5198–5202.
31 R. M. Jarvis and R. Goodacre, *Anal. Chem.*, 2004, **76**, 40–47.
32 P. Rosch, M. Harz, M. Schmitt, K. Peschke, O. Ronneberger, H. Burkhardt, H. Motzkus, M. Lankers, S. Hofer, H. Thiele and J. Popp, *Appl. Environ. Microbiol.*, 2005, **71**, 1626–1637.
33 W. Premasiri, D. Moir, M. Klempner, N. Krieger, G. Jones and L. Ziegler, *J. Phys. Chem. B*, 2005, **109**, 312–320.
34 S. Bell, J. Mackle and N. Sirimuthu, *Analyst*, 2005, **130**, 545–549.
35 X. Zhang, M. Young, O. Lyandres and R. V. Duyne, *J. Am. Chem. Soc.*, 2005, **127**, 4484–4489.
36 R. Goodacre, B. Shann, R. Gilbert, E. Timmins, A. McGovern, B. Alsberg, D. Kell and N. Logan, *Anal. Chem.*, 2000, **72**, 119–127.
37 T. A. Alexander, P. M. Pellegrino and J. B. Gillespie, *Appl. Spectrosc.*, 2003, **57**, 1340–1345.
38 A. E. Grow, L. L. Wood, J. L. Claycomb and P. A. Thompson, *J. Microbiol. Methods*, 2003, **53**, 221–233.
39 L. Shute, C. Gutteridge, J. Norris and R. Berkeley, *J. Gen. Microbiol.*, 1984, **130**, 343–355.
40 P. C. Lee and D. Meisel, *J. Phys. Chem.*, 1982, **86**, 3391–3395.
41 C. H. Munro, W. E. Smith, M. Garner, J. Clarkson and P. C. White, *Langmuir*, 1995, **11**, 3712–3720.
42 K. P. J. Williams, G. D. Pitt, D. N. Batchelder and B. J. Kip, *Appl. Spectrosc.*, 1994, **48**, 232–235.
43 K. P. J. Williams, G. D. Pitt, B. J. E. Smith, A. Whitley, D. N. Batchelder and I. P. Hayward, *J. Raman Spectrosc.*, 1994, **25**, 131–138.
44 R. Goodacre, É. M. Timmins, R. Burton, N. Kaderbhai, A. Woodward, D. B. Kell and P. J. Rooney, *Microbiology*, 1998, **144**, 1157–1170.
45 I. T. Jolliffe, *Principal Component Analysis*, Springer-Verlag, New York, 1986.
46 B. F. J. Manly, *Multivariate Statistical Methods: A Primer*, Chapman & Hall, London, 1994.
47 M. Seasholtz and B. Kowalski, *Anal. Chim. Acta*, 1993, **277**, 165–177.
48 R. Brereton, *Chemometrics: Data Analysis for the Laboratory and Chemical Plant*, 1st edn., John Wiley & Sons Ltd., Chichester, 2003.
49 J. A. Jernigan, D. S. Stephens, D. A. Ashford, C. Omenaca, M. S. Topiel, M. Galbraith, M. Tapper, T. L. Fisk, S. Zaki, T. Popovic, R. F. Meyer, C. P. Quinn, S. A. Harper, S. K. Fridkin, J. J. Sejvar, C. W. Shepard, M. McConnell, J. Guarner, W. J. Shieh, J. M. Malecki, J. L. Gerberding, J. M. Hughes and B. A. Perkins, *Emerg. Infectious Dis.*, 2001, **7**, 933–944.
50 S. Vaidyanathan, J. J. Rowland, D. B. Kell and R. Goodacre, *Anal. Chem.*, 2001, **73**, 4134–4144.
51 H. Susi, J. Sampugna, J. Hampson and J. Ard, *Biochemistry*, 1979, **18**, 297–301.
52 M. P. Doyle, L. R. Beuchat and T. J. Montville, American Society of Microbiology Press, Washington DC, 1997.
53 W. Barnaby, *The Plague Makers: The Secret World of Biological Warfare*, Vision Paperbacks, London, 1997.
54 F. Dollish, W. Fateley and F. Bentley, *Characteristic Raman Frequencies of Organic Compounds*, John Wiley & Sons Inc., New York, 1974.

